Subwavelength grating filtering devices

Junjia Wang,[1*] Ivan Glesk,[2] and Lawrence R. Chen[1]

[1] *Department of Electrical and Computer Engineering, McGill University, Montreal, QC H3A 0E9 Canada*
[2] *Department of Electronic and Electrical Engineering, University of Strathclyde, Glasgow, G1 1XU UK*
[*] *junjia.wang@mail.mcgill.ca*

Abstract: We propose and simulate the characteristics of optical filters based on subwavelength gratings. In particular, we demonstrate through numerical simulations the feasibility of implementing SWG Bragg gratings in silicon-on-insulator (SOI). We also propose SWG ring resonators in SOI and verify their operation using numerical simulations and experiments. The fabricated devices exhibit an extinction ratio as large as 30 dB and a Q-factor as high as ~20,000. These fundamental SWG filters can serve as building blocks for more complex devices.

OCIS codes: (050.2770) Gratings; (130.3120) Integrated optics devices; (130.7408) Wavelength filtering devices.

References and links

1. M. Lipson, "Silicon photonics: the optical spice rack," Electron. Lett. **45**, 575–577 (2009).
2. P. J. Bock, P. Cheben, J. H. Schmid, J. Lapointe, A. Delâge, S. Janz, G. C. Aers, D.-X. Xu, A. Densmore, and T. J. Hall, "Subwavelength grating periodic structures in silicon-on-insulator: a new type of microphotonic waveguide," Opt. Express **18**(19), 20251–20262 (2010).
3. D. J. Lockwood and L. Pavesi, *Silicon Photonics: Components and Integration, Vol. II* (Springer, 2011).
4. R. Halir, A. Ortega-Monux, J. H. Schmid, C. Alonso-Ramos, J. Lapointe, D. X. Xu, J. G. Wanguemert-Perez, I. Molina-Fernandez, and S. Janz, "Recent advances in silicon waveguide devices using sub-wavelength gratings," IEEE J Sel Top Quant **20**(4) 8201313 (2014).
5. R. Halir, P. Cheben, J. H. Schmid, R. Ma, D. Bedard, S. Janz, D. X. Xu, A. Densmore, J. Lapointe, and I. Molina-Fernández, "Continuously apodized fiber-to-chip surface grating coupler with refractive index engineered subwavelength structure," Opt. Lett. **35**(19), 3243–3245 (2010).
6. P. J. Bock, P. Cheben, J. H. Schmid, J. Lapointe, A. Delâge, D.-X. Xu, S. Janz, A. Densmore, and T. J. Hall, "Subwavelength grating crossings for silicon wire waveguides," Opt. Express **18**(15), 16146–16155 (2010).
7. P. J. Bock, P. Cheben, J. H. Schmid, A. Delâge, D.-X. Xu, S. Janz, and T. J. Hall, "Sub-wavelength grating mode transformers in silicon slab waveguides," Opt. Express **17**(21), 19120–19133 (2009).
8. A. Ortega-Monux, L. Zavargo-Peche, A. Maese-Novo, I. Molina-Fernández, R. Halir, J. Wanguemert-Perez, P. Cheben, and J. Schmid, "High-performance multimode interference coupler in silicon waveguides with subwavelength structures," IEEE Photon. Technol. Lett. **23**(19), 1406–1408 (2011).
9. A. V. Velasco, M. L. Calvo, P. Cheben, A. Ortega-Moñux, J. H. Schmid, C. A. Ramos, Í. M. Fernandez, J. Lapointe, M. Vachon, S. Janz, and D. X. Xu, "Ultracompact polarization converter with a dual subwavelength trench built in a silicon-on-insulator waveguide," Opt. Lett. **37**(3), 365–367 (2012).
10. X. Wang, W. Shi, H. Yun, S. Grist, N. A. F. Jaeger, and L. Chrostowski, "Narrow-band waveguide Bragg gratings on SOI wafers with CMOS-compatible fabrication process," Opt. Express **20**(14), 15547–15558 (2012).
11. L. Chrostowski, S. Grist, J. Flueckiger, W. Shi, X. Wang, E. Ouellet, H. Yun, M. Webb, B. Nie, Z. Liang, K. C. Cheung, S. A. Schmidt, D. M. Ratner, and N. A. F. Jaeger, "Silicon photonic resonator sensors and devices," Proc. SPIE **8236**, 823620 (2012).
12. W. Bogaerts, P. De Heyn, T. Van Vaerenbergh, K. De Vos, S. K. Selvaraja, T. Claes, P. Dumon, P. Bienstman, D. Van Thourhout, and R. Baets, "Silicon microring resonators," Laser Photon Rev **6**(1), 47–73 (2012).
13. J. Y. Lee and P. M. Fauchet, "Slow-light dispersion in periodically patterned silicon microring resonators," Opt. Lett. **37**(1), 58–60 (2012).
14. S. M. Rytov, "Electromagnetic properties of a finely stratified medium," Sov Phys Jetp-Ussr **2**, 466–475 (1956).
15. P. Lalanne and J. P. Hugonin, "High-order effective-medium theory of subwavelength gratings in classical mounting: application to volume holograms," J. Opt. Soc. Am. A **15**(7), 1843–1851 (1998).
16. P. Yeh, *Optical Waves in Layered Media* (Wiley, 1988).
17. K. E. Oughstun and N. A. Cartwright, "On the Lorentz-Lorenz formula and the Lorentz model of dielectric dispersion," Opt. Express **11**(13), 1541–1546 (2003).
18. R. Kashyap, *Fiber Bragg Gratings* (Academic Press, 1999).
19. K. O. Hill and G. Meltz, "Fiber Bragg grating technology fundamentals and overview," J. Lightwave Technol. **15**(8), 1263–1276 (1997).

#208807 - $15.00 USD Received 25 Mar 2014; revised 11 May 2014; accepted 10 Jun 2014; published 17 Jun 2014

20. G. D. Marshall, M. Ams, and M. J. Withford, "Direct laser written waveguide-Bragg gratings in bulk fused silica," Opt. Lett. **31**(18), 2690–2691 (2006).
21. I. Giuntoni, A. Gajda, M. Krause, R. Steingrüber, J. Bruns, and K. Petermann, "Tunable Bragg reflectors on silicon-on-insulator rib waveguides," Opt. Express **17**(21), 18518–18524 (2009).
22. T. E. Murphy, J. T. Hastings, and H. I. Smith, "Fabrication and characterization of narrow-band Bragg-reflection filters in silicon-on-insulator ridge waveguides," J. Lightwave Technol. **19**(12), 1938–1942 (2001).
23. S. J. Xiao, M. H. Khan, H. Shen, and M. H. Qi, "A highly compact third-order silicon microring add-drop filter with a very large free spectral range, a flat passband and a low delay dispersion," Opt. Express **15**(22), 14765–14771 (2007).
24. Q. F. Xu, B. Schmidt, S. Pradhan, and M. Lipson, "Micrometre-scale silicon electro-optic modulator," Nature **435**(7040), 325–327 (2005).
25. F. F. Liu, Q. Li, Z. Y. Zhang, M. Qiu, and Y. K. Su, "Optically tunable delay line in silicon microring resonator based on thermal nonlinear effect," Ieee J Sel Top Quant **14**(3), 706–712 (2008).
26. J. Cardenas, M. A. Foster, N. Sherwood-Droz, C. B. Poitras, H. L. R. Lira, B. B. Zhang, A. L. Gaeta, J. B. Khurgin, P. Morton, and M. Lipson, "Wide-bandwidth continuously tunable optical delay line using silicon microring resonators," Opt. Express **18**(25), 26525–26534 (2010).
27. L. Zavargo-Peche, A. Ortega-Monux, J. G. Wanguemert-Perez, and I. Molina-Fernandez, "Fourier based combined techniques to design novel sub-wavelength optical integrated devices," Prog. Electromagnetics Res. **123**, 447–465 (2012).
28. Q. F. Xu, D. Fattal, and R. G. Beausoleil, "Silicon microring resonators with 1.5-microm radius," Opt. Express **16**(6), 4309–4315 (2008).
29. L. Chrostowski, and M. Hochberg, *Silicon Photonics Design* (Lulu, 2013).
30. J. K. S. Poon, J. Scheuer, Y. Xu, and A. Yariv, "Designing coupled-resonator optical waveguide delay lines," J. Opt. Soc. Am. B **21**(9), 1665–1673 (2004).

1. Introduction

There is a growing need to develop integrated components to perform a variety of signal processing functions for optical communications applications. Over the past few years, the development of active and passive devices in silicon photonics has been the subject of intense research and a number of enabling technologies have been demonstrated [1]. One specific device that has attracted interest due to its unique properties is the subwavelength grating (SWG). An SWG is based on a periodic arrangement between two different materials with a period much smaller than the wavelength of the light. A new type of microphotonic waveguide based on a SWG was proposed and demonstrated [2] as a possible means of reducing propagation loss [3]. In theory, the structure is lossless. In practice, the measured loss is found to be as low as 2.1 dB/cm with negligible wavelength dependent loss. SWGs also offer high flexibility in terms of tailoring the effective index and dispersion. The SWG enables a whole new platform for silicon photonics and indeed, a variety of devices have been investigated and demonstrated [4]. These include fiber-to-chip surface grating couplers which reduce coupling loss to optical fibers [5]; SWG crossings, which can be used to reduce the footprint of integrated devices [6]; mode transformers, which can be used for butt coupling and mode conversions [7]; MMI couplers with improvements both in size and bandwidth [8]; and a polarization converter [9] with a dual subwavelength trench, which supports two hybrid modes and reduces device length. All of these devices (except for the polarization converter) can be fabricated with a single-etch process.

Optical filters are key components for a wide range of applications in optical communications and sensing and those based on Bragg gratings and ring resonators have been studied thoroughly in SOI [10–13]. However, there have been no reports of SWG filters. In this paper, we propose and demonstrate two different types of SWG filters in SOI: SWG Bragg gratings and SWG ring resonators. We use 2.5D FDTD simulations to calculate the spectral responses of the Bragg grating and ring resonator filters and also present experimental results for the SWG ring resonators. These filters may be desirable as fundamental building blocks that can be integrated with existing SWG devices to develop more complex structures that provide increased functionality such as optical add/drop multiplexers.

#208807 - $15.00 USD Received 25 Mar 2014; revised 11 May 2014; accepted 10 Jun 2014; published 17 Jun 2014

2. SWGs on SOI

An SWG is defined generally as a grating structure with a period that is smaller than the wavelength of light. It is formed by a sequence of alternating media with high and low refractive indices n_1 and n_2, respectively, with period Λ along the direction of propagation (the corresponding widths of the high and low refractive index media are a and Λ - a, respectively, as shown in Fig. 1).

The unique property of an SWG is that its dispersion is almost linear over a certain range of wavelengths [14]. In other words, the SWG is a waveguide (of the same transverse dimensions) with a uniform effective index along the propagation direction [2, 14, 15]. Wave propagation in SWGs can be modeled in terms of Bloch waves where each Bloch mode has a specific wave number [16]. By choosing the duty cycle $f = a/\Lambda$, the effective index of the SWG waveguide can be modified and hence, the propagation properties (i.e., of the Bloch mode) can be controlled.

In SOI, the SWG waveguides can be realized by alternating periodically segments of silicon and silica [2]. A schematic of an SWG waveguide is shown in Fig. 1: the silicon SWG waveguide (with cross-sectional dimensions $W \times h$) sits on top of a buried (or bottom) oxide (BOX) layer and is covered by an index-matched silica cladding layer. Two SWG tapers, also shown in Fig. 1, are used to convert light into (and from) a Bloch mode before (and after) propagating through the SWG waveguide [2].

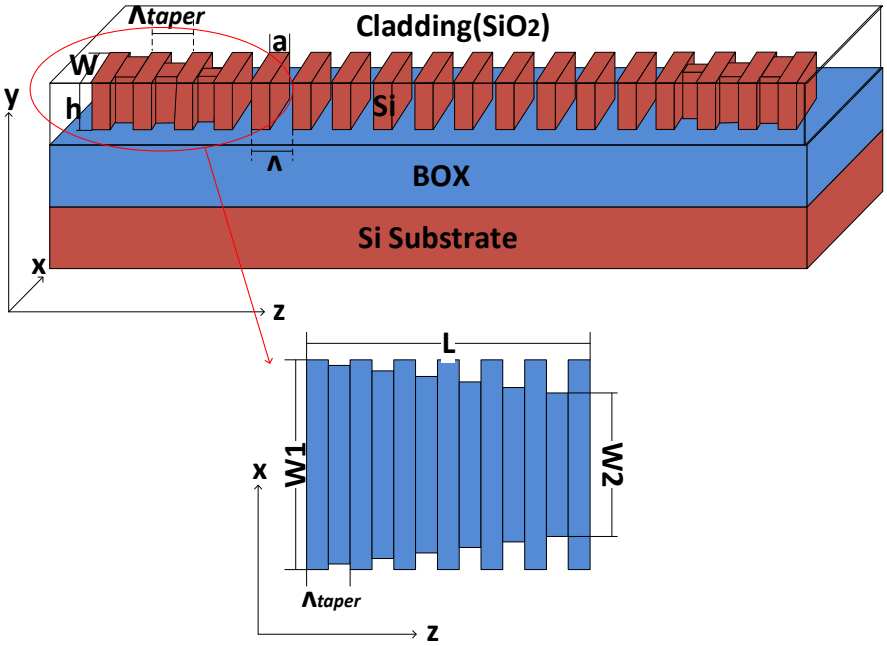

Fig. 1. SWG waveguide in SOI and top view of the SWG taper.

For illustrative purposes, we consider a BOX thickness of 3 μm and a silica cladding thickness of 2 μm; the SWG period is $\Lambda = 300\,\text{nm}$ with a duty cycle of $f = a/\Lambda = 0.5$ and a cross-section $W \times h$ of 450 nm × 220 nm. All of these values are typical of SOI fabrication processes. The SWG taper is based on the parameters described in [2], since the SWG dimensions are similar: Λ_{taper} = 200 nm and the waveguide width is varied from W_1 = 450 nm down to W_2 = 100 nm over a length of 15 μm.

In what follows, all simulations of the SWG filters are performed using Lumerical MODE, a 2.5D FDTD simulation software. The 2.5D FDTD simulations are suitable since

#208807 - $15.00 USD Received 25 Mar 2014; revised 11 May 2014; accepted 10 Jun 2014; published 17 Jun 2014

the SWG devices are invariant in one dimension (i.e., along the *y* axis). While 2.5D FDTD simulations are not as robust as their full 3D FDTD counterparts for obtaining exact quantitative results, they are less computationally intensive and can be used to guide the design of SWG devices and to understand general trends in device characteristics and properties. We use wavelength dependent refractive indices for Si and SiO_2 based on a Lorentz model [17] which is compatible with FDTD simulations. The mesh resolution is auto-nonuniform with a mesh accuracy index of 4 as defined in Lumerical. The space discretization depends on the specific wavelength, but Δx and Δz are ~10 nm. The simulation time step is Δt = 0.05 fs and the wavelength resolution is 20 pm. We use a simulation window of 60 ps for SWG Bragg grating devices and 50 ps for SWG ring resonator devices. The perfectly matched layer boundaries are located at more than twice the dimension of the device being simulated along the *x* and *y* axes, and an additional 10 μm away from the ends of device along the *z* axis.

3. SWG filters

3.1 SWG Bragg gratings

Bragg gratings are one of the most common devices used in optical communications for applications such as filtering, add/drop multiplexing, and dispersion compensation. Significant research efforts have been devoted to the study of fiber Bragg gratings [18, 19], waveguide Bragg gratings [20], and Bragg gratings on SOI [10, 21, 22]. As described in Section 2, the effective index of an SWG waveguide depends on the duty cycle. As such, an SWG Bragg grating can be realized by interleaving two SWG waveguides as illustrated in Fig. 2. We define two duty cycles f_1 and f_2 as $f_1 = a/\Lambda_1$ and $f_2 = a/\Lambda_2$, and the SWG Bragg grating has a period of $\Lambda_1 + \Lambda_2$; by varying f_1 and f_2, we create a periodic variation in the effective index and can thus obtain Bragg reflection.

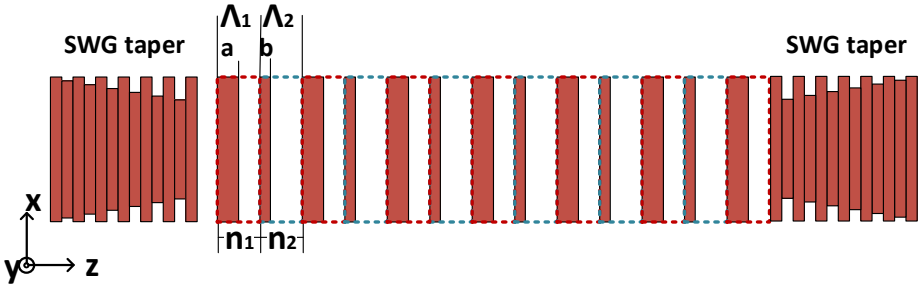

Fig. 2. Schematic of an SWG Bragg grating.

To verify the principle of operation, we simulate the spectral responses of different SWG Bragg grating structures. The waveguide parameters we used are those described in Section 2. Figure 3 shows the transmission and reflection spectra of SWG Bragg gratings constructed using f_1 = 50% and different values of f_2. Λ_1 and Λ_2 are both kept at 300 nm so that the period of the SWG Bragg grating is 600 nm. Clearly, a reflection peak (transmission notch) is obtained within the SWG transmission passband. Moreover, the reflection peak (Bragg wavelength) shifts to longer wavelengths as f_2 is increased (which is equivalent to increasing the effective index). Note that the transmission passbands of the SWG shift in wavelength due to the changes in the effective duty cycle and hence effective index. Table 1 summarizes the variation in Bragg wavelength as a function of f_2. The additional reflection peak at 1405.3 nm in Fig. 3(c) is due to a higher-order Bloch mode, which has a corresponding effective index of 1.171. Table 2 shows the simulated effective indices of the fundamental and higher-order

#208807 - $15.00 USD Received 25 Mar 2014; revised 11 May 2014; accepted 10 Jun 2014; published 17 Jun 2014

Bloch modes for the SWG Bragg gratings. The reflection bandwidth can be controlled by adjusting the length of the SWG waveguide (or number of grating segments), as shown in Table 3 (as mentioned previously, the specific values of Bragg wavelength, effective indices of the Bloch modes, or 3 dB bandwidth may not be exact due to the use of 2.5D FDTD simulations; however, the main purpose here is to understand how varying the different parameters can impact the Bragg grating properties). The SWG Bragg gratings can provide bandwidths achievable with conventional Bragg gratings in SOI [10, 21, 22]; the main advantage of SWG structures is the possibility of a single etch fabrication process, which may reduce fabrication cost and time.

Table 1. Bragg wavelength for different values of duty cycle f_2

f_1	f_2	Bragg Wavelength
50%	40%	1574.22 nm
50%	46.67%	1592.62 nm
50%	53.33%	1610.15 nm
50%	60%	1626.75 nm

Table 2. Effective indices of Bloch modes for different duty cycles

f_1	f_2	Bloch mode 1	Bloch mode 2
50%	40%	1.312	1.156
50%	46.67%	1.328	1.163
50%	53.33%	1.342	1.171
50%	60%	1.355	1.177

Table 3. Reflection bandwidth (3 dB) for SWG Bragg gratings with different number of segments

f_1	f_2	3 dB Bandwidth with 2,000 segments	3 dB Bandwidth with 4,000 segments
50%	40%	0.95 nm	0.37 nm
50%	46.67%	1.00 nm	0.62 nm
50%	53.33%	1.01 nm	0.64 nm
50%	60%	1.09 nm	0.47 nm

#208807 - $15.00 USD Received 25 Mar 2014; revised 11 May 2014; accepted 10 Jun 2014; published 17 Jun 2014

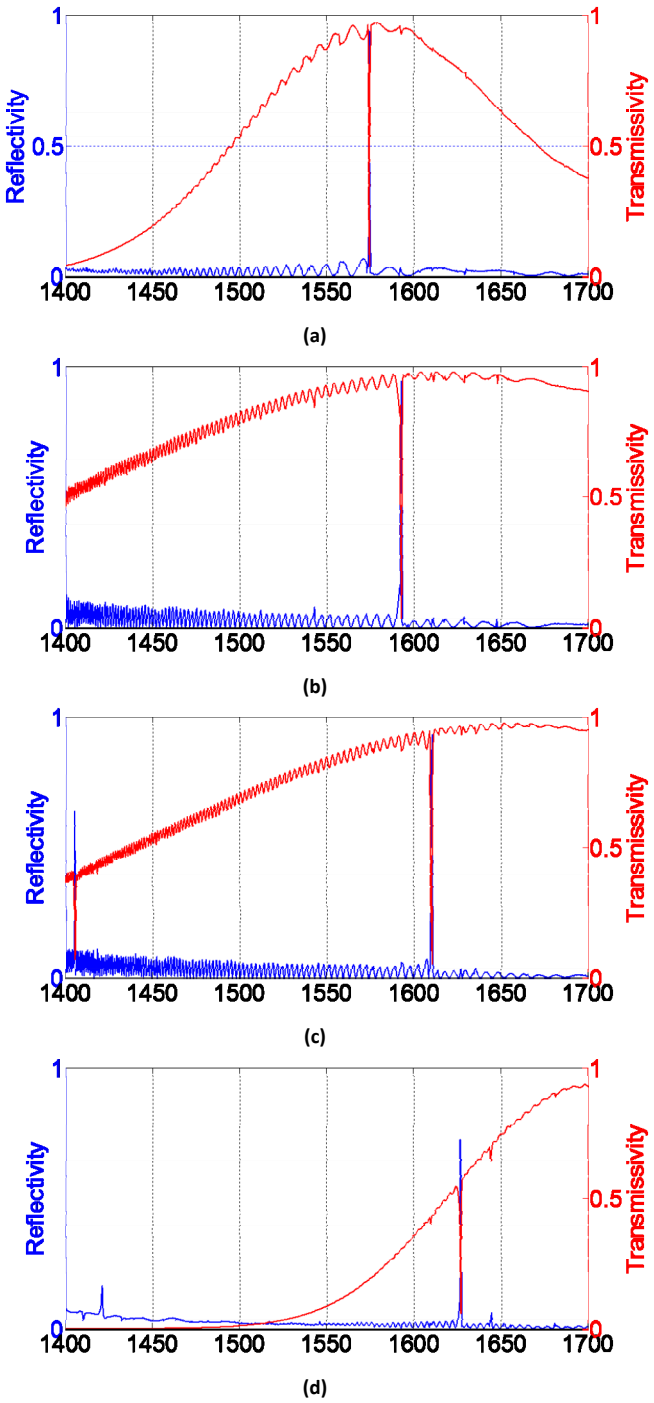

Fig. 3. Transmission and reflection spectra of SWG Bragg gratings for (a) $f_1 = 50\%$, and $f_2 = 40\%$, (b) $f_1 = 50\%$, and $f_2 = 46.67\%$, (c) $f_1 = 50\%$, and $f_2 = 53.33\%$, and (d) $f_1 = 50\%$, and $f_2 = 60\%$.

#208807 - $15.00 USD Received 25 Mar 2014; revised 11 May 2014; accepted 10 Jun 2014; published 17 Jun 2014

3.2 SWG ring resonator

In addition to Bragg gratings, ring resonators are also very effective wavelength-selective devices. A variety of ring resonator-based devices in SOI have been demonstrated, including filters [23], modulators [24], and slow light structures/tunable-delay lines [25, 26]. We now investigate the feasibility of SWG-based ring resonators and consider an add-drop configuration comprising two SWG waveguides and an SWG ring waveguide as illustrated in Fig. 4.

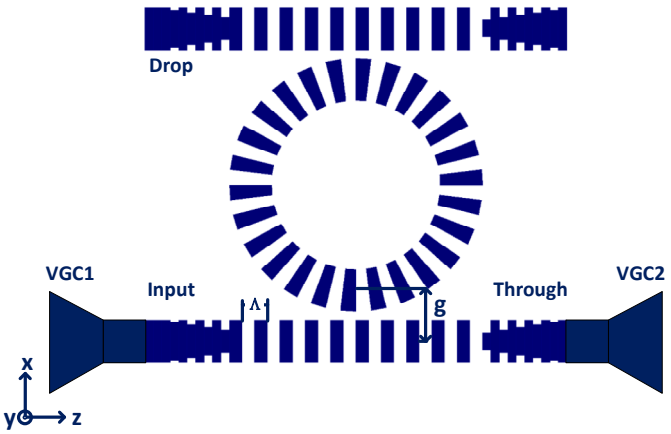

Fig. 4. Schematic of the SWG ring resonator. VGC: vertical grating coupler.

The coupler between the SWG waveguide and ring is similar to that presented in [27] (though the coupling length is short and not uniform), with a gap (g) of 550 nm. Again, the period of the SWG waveguide is 300 nm and the transverse dimensions are $W \times h = 450\,\text{nm} \times 220\,\text{nm}$. In the SWG ring region, the period is roughly 300 nm as well, but this depends on the position of the segments as the SWG ring is sliced by degrees. For instance, for an SWG ring with 10 μm radius, two adjacent segments are separated by 0.015 radians according to the center, and the width of the segments is approximately equal to the length of the arc with a 0.015 radians of central angle. The smallest gap in the design is 100 nm, which can be fabricated readily using both deep UV and e-beam lithography.

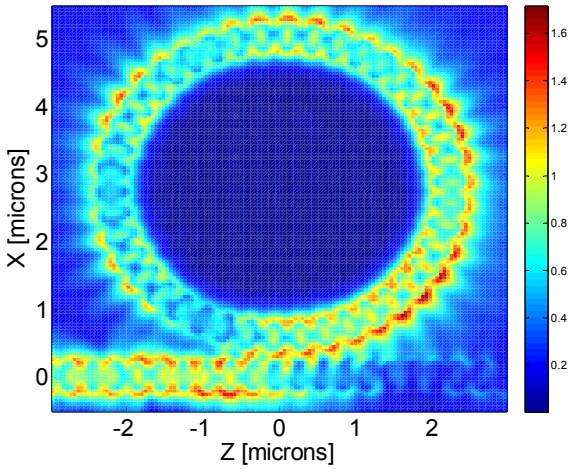

Fig. 5. Top view of the E-field propagating in the SWG ring resonator.

#208807 - $15.00 USD Received 25 Mar 2014; revised 11 May 2014; accepted 10 Jun 2014; published 17 Jun 2014

Figure 5 shows a top view of the field propagating in the SWG ring resonator. The SWG preserves Bloch mode propagation in both the waveguide and the ring regions. Figure 6(a) shows the spectral responses of the SWG ring resonator with a ring radius of 10 µm. The free spectral range (FSR) is 20 nm and the 3 dB bandwidth is 0.3 nm at 1682.3 nm. The corresponding *Q*-factor is ~5,600 and the extinction ratio (ER) is 16 dB. Figure 6(b) shows the spectral responses of the SWG ring resonator when the ring radius is increased to 15 µm. The FSR has decreased (as expected for larger rings) to 13.6 nm and the 3 dB bandwidth is 0.15 nm at 1614.4 nm. The corresponding *Q*-factor is ~10,760 and the ER is 17.2 dB.

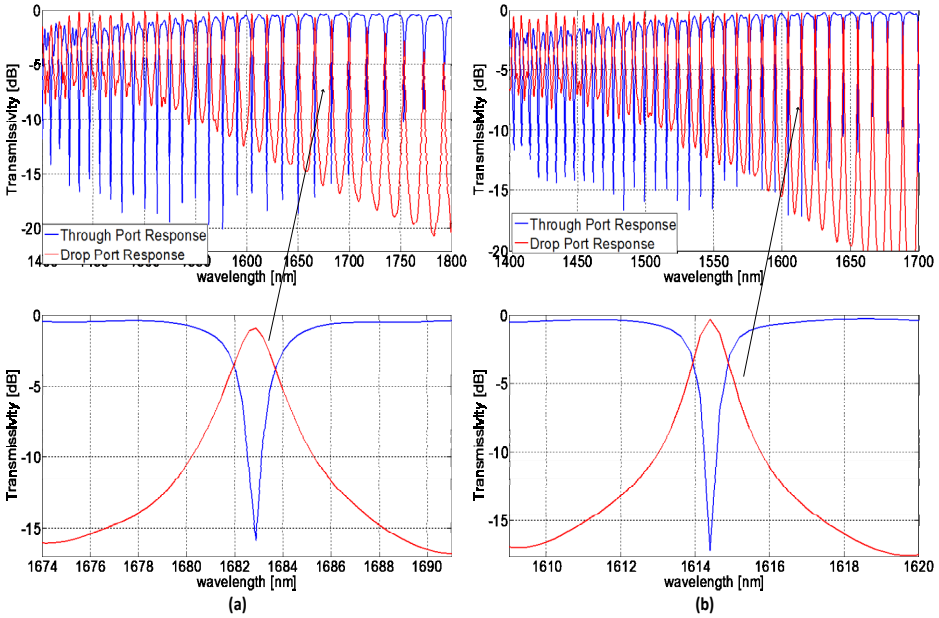

Fig. 6. Spectral response of an SWG ring resonator with (a) 10 µm radius, (b) 15 µm radius.

To demonstrate experimentally the SWG ring resonators, a set of devices were fabricated at the University of Washington Nanofabrication Facility (WNF) using electron beam lithography and a full etch with top oxide cladding. The device parameters are similar to those used in the simulations: the Si waveguide thickness (i.e., *h*) is 220 nm on top of a 3 µm BOX layer on a Si substrate. The waveguide width *W* is 500 nm, the SWG grating period is 300 nm, and the gap g = 600 nm. The SWG taper has a period of 200 nm, and the width varies from W_1 = 500 nm down to W_2 = 200 nm over a length of 15 µm. Vertical grating couplers (VGCs) are used to couple light into and out of the ring resonators and are optimized for TE transmission. A tunable laser (scanned in steps of 10 pm or 1 pm) and an optical power meter are used to measure the spectral responses. All of the results are normalized to the transmission response of the VGCs (characterized separately via transmission measurements through a short length of strip waveguide). The measured total fiber-to-fiber loss at a wavelength of 1600 nm is ~42 dB. From measurements of simple test waveguides, the estimated propagation loss in the SWG waveguide is 3 dB/cm. Figure 7(a) shows the measured transmission spectrum for an SWG ring resonator with a ring radius of 10 µm. The FSR is 16.3 nm and at 1616.4 nm, the ER is ~30 dB. The inset shows a zoom near a resonance measured with 1 pm resolution. The corresponding Q-factor (defined as $\lambda_0/\Delta\lambda$ where λ_0 is the central wavelength and $\Delta\lambda$ is the 3 dB bandwidth of a resonance [28]) is measured to be ~8,833. Figure 7(b) shows the response for a ring radius of 15 µm. The FSR has decreased to 11.1 nm as expected for larger rings [12]. At 1631.9 nm, the measured ER and Q-factor are ~23 dB and 20,400. Finally, Fig. 7(c) illustrates the response of an SWG ring

#208807 - $15.00 USD Received 25 Mar 2014; revised 11 May 2014; accepted 10 Jun 2014; published 17 Jun 2014

resonator with a ring radius of 20 µm. The FSR is ~7.5 nm and at 1586.1 nm, the ER is ~13 dB and the Q-factor is ~7,930.

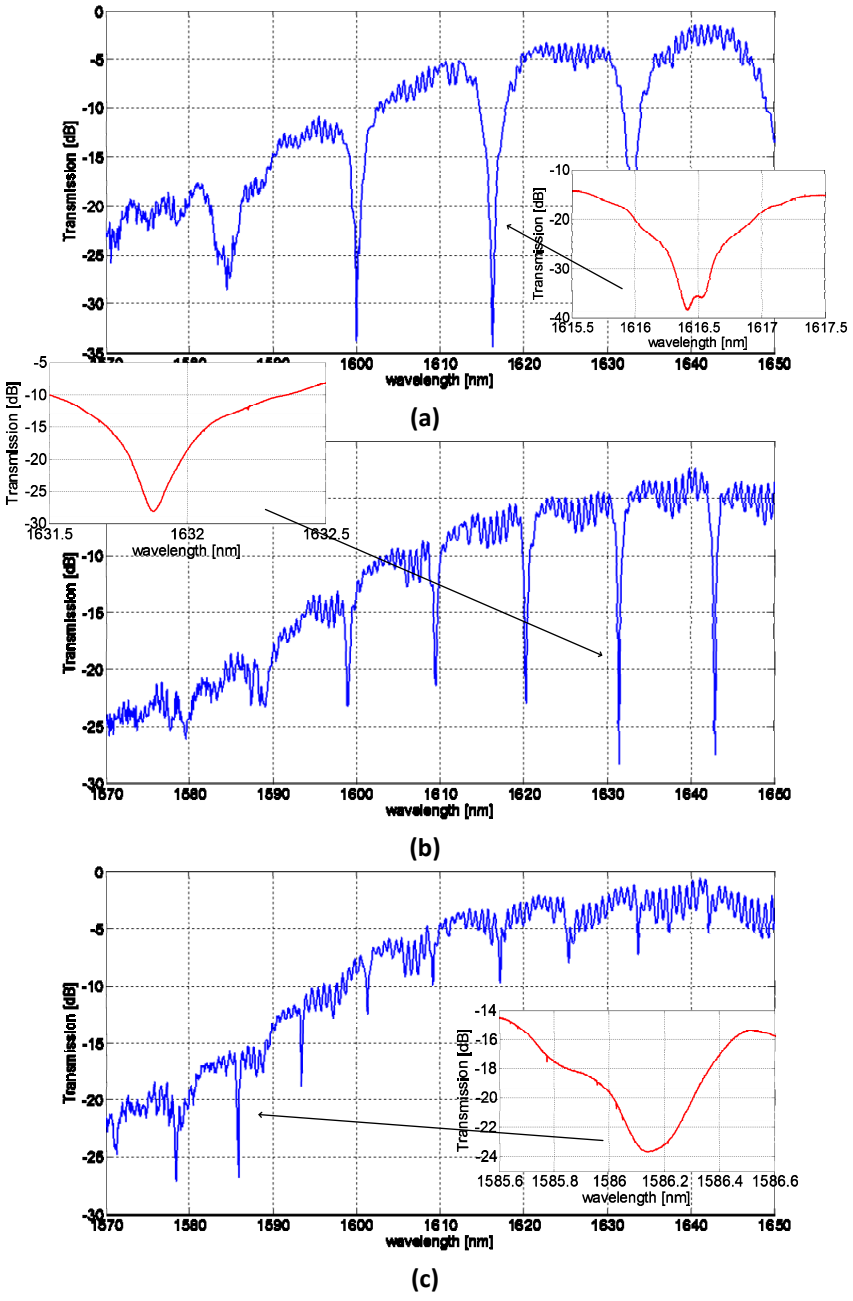

Fig. 7. Measured transmission spectra (10 pm resolution) of SWG ring resonators with a ring radius of (a) 10 µm, (b) 15 µm, and (c) 20 µm. The insets show a zoom of a single resonance measured with 1 pm resolution.

The ER can be further improved using a race-track configuration [12] as illustrated in Fig. 8. Figure 9 shows the simulated spectral responses of SWG race-track ring resonators with a

#208807 - $15.00 USD Received 25 Mar 2014; revised 11 May 2014; accepted 10 Jun 2014; published 17 Jun 2014

radius of 10 μm and 15 μm, where the lengths of the coupling sections (denoted *L*) are also 10 μm and 15 μm, respectively. The SWG waveguide period and the gap *g* are the same as those used for simulating the 'conventional' SWG ring resonators. Within the limitations of the 2.5D FDTD simulations, the ER of the resonators can be improved to over 30 dB and 20 dB, respectively.

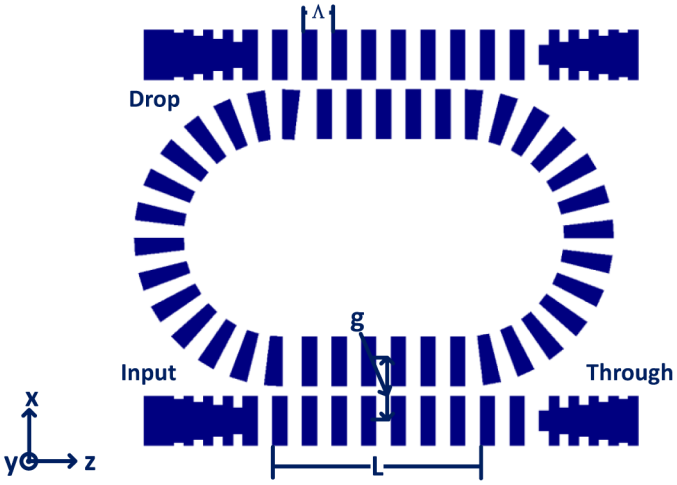

Fig. 8. Schematic of an SWG race-track ring resonator.

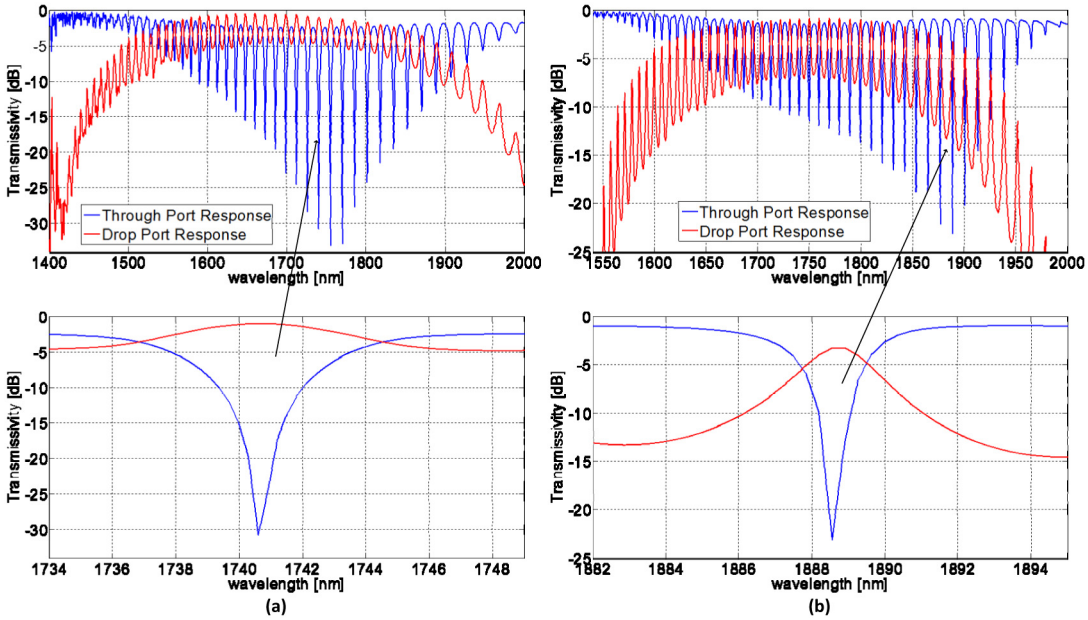

Fig. 9. Spectral responses of SWG race-track ring resonator with (a) 10 μm radius, and (b) 15 μm radius.

By comparing simulation results with conventional SOI ring resonators of the same transverse dimensions, the SWG ring resonators achieve better ER. More importantly, the coupling cross-over length is shorter using SWG waveguides as shown in Fig. 10; as such, more compact devices can be fabricated.

#208807 - $15.00 USD Received 25 Mar 2014; revised 11 May 2014; accepted 10 Jun 2014; published 17 Jun 2014

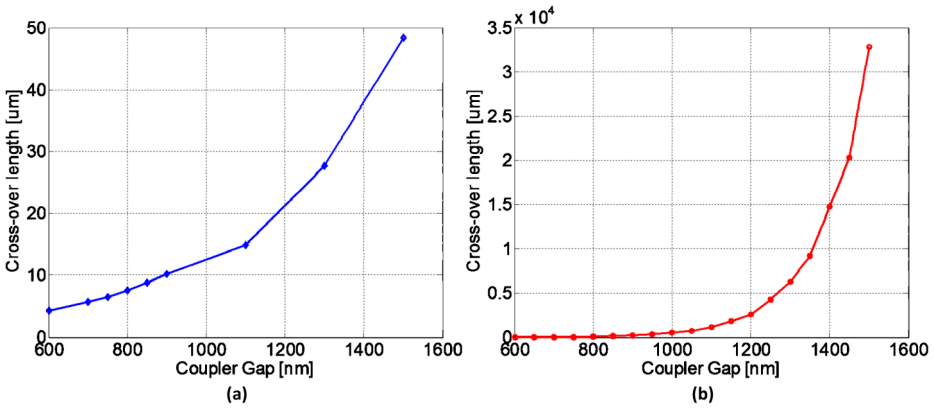

Fig. 10. Cross-over length versus gap of the coupler at a wavelength of 1550 nm: (a) SWG (b) directional coupler in Si [29].

4. Discussion and summary

In this paper, we have demonstrated the feasibility of two types of SWG filters. By taking advantage of the ability to tailor the effective index of SWG waveguides, we proposed filters based on SWG Bragg gratings and ring resonators. For SWG Bragg gratings, the peak reflection wavelength can be tuned by adjusting the duty cycle of the interleaved SWG waveguides. The fabrication of SWG Bragg gratings involves only a single etch process, which reduces both fabrication cost and time compared to the fabrication processes used in [10, 21, 22] for conventional Bragg gratings in SOI. We also designed and experimentally demonstrated SWG ring resonators. The fabricated devices exhibit ERs and Q-factors that are comparable to conventional ring resonators in SOI. The SWG structures, however, offer the possibility for greater compactness, especially for race-track configurations which typically have higher ER. Using the single ring as a building block, double ring configurations or coupled-resonator optical waveguides (CROW) can also be realized, which can be used to achieve higher ER and reconfigurable delay lines [30]. Both SWG Bragg gratings and ring resonators are single etch devices, which ease the fabrication process. They have shot pitches larger than 100 nm, which is compatible with DUV and e-beam lithography. With these filtering devices mentioned above, more exciting devices can be realized based on the SWG platform.

Acknowledgments

This work was supported by the NSERC NGON CREATE program and the Royal Society under the International Exchanges Scheme 2012/R2. The SWG ring resonators were fabricated by Richard Bojko at the University of Washington Nanofabrication Facility (WNF), a member of the NSF National Nanotechnology Infrastructure Network.